Magnetic structures of RbCuCl$_3$ in a transverse field

A. E. Jacobs and T. Nikuni

Department of Physics, University of Toronto, Toronto, Ontario, Canada M5S 1A7

(Received 8 November 2001; published 16 April 2002)

A recent high-field magnetization experiment found a phase transition of unknown character in the layered, frustrated antiferromagnet RbCuCl$_3$, in a transverse field (in the layers). Motivated by these results, we have examined the magnetic structures predicted by a model of RbCuCl$_3$, using the classical approximation. At small fields, we obtain the structure already known to be optimal, an incommensurate (IC) spiral with wave vector **q** in the layers. At higher fields, we find a staircase of long-period commensurate (C) phases (separated initially by the low-field IC phase), then two narrow IC phases, then a fourth IC phase (also with intermediate C phases), and finally the ferromagnetically aligned phase at the saturation field H_S. The three-sublattice C states familiar from the theory of the triangular antiferromagnet are never optimal. The C phases and the two intermediate IC phases were previously unknown in this context. The magnetization is discontinuous at a field $\approx 0.4 H_S$, in qualitative agreement with experiment, though we find much fine structure not reported.

I. INTRODUCTION

The ABX_3 family of layered compounds has been studied extensively for several decades.[1] Much of this interest arises because the frustrated antiferromagnetic interactions in the a-b layers give rise to unusual magnetic properties. Quantum and thermal fluctuations can have exceptionally large effects in these materials; for example, the stacked triangular antiferromagnet (TAFM) CsCuCl$_3$ exhibits novel fluctuation-induced magnetic phase transitions in both a longitudinal field[2,3] (in the c direction, normal to the layers) and a transverse field.[4–6]

RbCuCl$_3$, another frustrated antiferromagnet of the ABX_3 family, is magnetically ordered for temperatures T less than $T_N \approx 19$ K;[7] the saturation field H_S (above which the ferromagnetically aligned phase is stable) is inconveniently large however (≈ 66 T).[8] Like CsCuCl$_3$, RbCuCl$_3$ is ferromagnetically stacked (in the c direction) and it has an incommensurate (IC) structure in zero field.[9] The Cu^{2+} ions in the a-b planes of RbCuCl$_3$ do not however form a regular triangular lattice. A room-temperature structural phase transition[10,11] distorts the structure, yielding a spatially anisotropic intraplane exchange, as shown in Fig. 1. As a result, at zero field the spins do not adopt the familiar three-sublattice, 120° structure of the TAFM; the structure is instead an IC helical structure along the b direction with a rotation angle 108° between adjacent spins.[12]

A neutron-diffraction experiment[9] at $T=1.6$ K in zero field found that the spins lie in the a-b planes and are ferromagnetically aligned in the c direction. The magnetic properties in large external field were recently investigated by means of magnetization measurements and by electron-spin resonance.[8] A discontinuity was found in the magnetization at a transverse field of $H=21.2$ T ($\approx 0.32 H_S$). The nature of this field-induced magnetic transition and the structure of the high-field state could however not be determined in these experiments.

The following reports theoretical results for spin structures of RbCuCl$_3$ in a transverse magnetic field. We use the simplest model Hamiltonian and investigate it analytically and numerically within the classical approximation. In the field range below H_S, solution of the Euler-Lagrange equations yields four IC phases, and in addition many long-period commensurate (C) phases in both the low-field and high-field regions; the three-sublattice C states of the TAFM are never optimal. Of these C and IC phases, only the low-field IC (helical) phase and the high-field IC (fan) phase were known previously;[13] the two intermediate IC phases occupy however only a very small field range. The magnetization is discontinuous, in qualitative agreement with experiment; the discontinuity occurs however at $H=0.41 H_S$, rather than at $0.32 H_S$ as observed, and the magnetization shows additional fine structure.

II. MODEL HAMILTONIAN

The model Hamiltonian describing RbCuCl$_3$ in a transverse magnetic field (which we take to lie in the x direction, to be explicit) is[8]

$$\mathcal{H} = -\sum_{in} 2J_0 \mathbf{S}_{in} \cdot \mathbf{S}_{in+1} - \sum_{in} 2\Delta J_0 S_{in}^z S_{in+1}^z$$
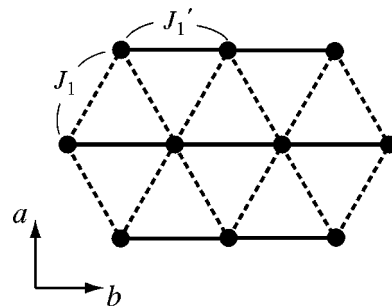$$- \sum_{\langle ij \rangle, n} 2J_1^{ij} \mathbf{S}_{in} \cdot \mathbf{S}_{jn} - g\mu_B H \sum_{in} S_{in}^x. \tag{1}$$

FIG. 1. The exchange interactions J_1 (broken lines) and J_1' (solid lines) in the distorted triangular lattice in the a-b plane.

65 174405-1

The x and z axes are taken along the a and c directions, respectively; $\mathbf{S}_{in}$ is the spin operator ($S = \frac{1}{2}$) of the ith Cu^{2+} site in the nth a-b plane, and the $\langle ij \rangle$ sum runs over nearest-neighbor sites in the a-b plane. The first term in Eq. (1) is the nearest-neighbor ferromagnetic exchange interaction ($J_0 > 0$) in the c direction; the second, with $\Delta J_0 < 0$, describes an anisotropy of easy-plane type. The third term, with $J_1^{ij} < 0$, is the antiferromagnetic exchange interaction in the a-b planes. As shown in Fig. 1, J_1^{ij} is anisotropic; $J_1^{ij} = -J_1'$ along the b direction while $J_1^{ij} = -J_1$ in the other two directions. The fourth and last term is the Zeeman energy. The parameters in Eq. (1) are $J_0 = 25.7$ K, $\Delta J_0 = -0.45$ K, $J_1 = 10.6$ K, $J_1' = 17.4$ K, and $g = 2.14$ (for $H \perp c$).

We investigate this Hamiltonian in the classical approximation. The spin operators $\mathbf{S}_{in}$ then become classical vectors of length $\frac{1}{2}$, and the Hamiltonian becomes an energy function; the ground-state spin structures are those that minimize the energy. The classical ground state of Eq. (1) in zero field is the helical structure[13]

$$\mathbf{S}_{in} = S\hat{\mathbf{x}}\cos(\mathbf{q}\cdot\mathbf{r}_{in}) + S\hat{\mathbf{y}}\sin(\mathbf{q}\cdot\mathbf{r}_{in}); \quad (2)$$

the easy-plane anisotropy favors spins in the a-b planes. The optimal wave vector is $\mathbf{q} = (0, q_0, 0)$, with $\cos q_0 = -J_1/2J_1'$; the above parameter values give $q_0/2\pi = 0.2993$.

In the special case $J_1' = J_1$, Eq. (1) reduces to the Hamiltonian of the stacked TAFM. Classically, the TAFM ground states are three-sublattice structures; they evolve continuously with field H, from the zero-field 120° structure (with $q_0/2\pi = 1/3$ in the above picture) up to the aligned state at H_S. These states are continuously degenerate at all $H < H_S$; energy minimization gives only two relations for the three angles ϕ_i between the sublattice spins and the field, namely,

$$\cos\phi_1 + \cos\phi_2 + \cos\phi_3 = g\mu_B H/(6J_1 S) \quad (3)$$

and $\Sigma_{i=1}^3 \sin\phi_i = 0$. This degeneracy, which is nontrivial, is broken in an identical manner by thermal and quantum fluctuations omitted in the classical approximation.[14,15]

We determine the spin structures of $RbCuCl_3$ in transverse fields with the help of three reasonable assumptions: the spins remain in the a-b planes, they are aligned ferromagnetically along the c direction, and they are aligned ferromagnetically also along the a direction. The last assumption is based on the fact that, along the a direction, the spins are coupled only through the J_1' exchange interaction. We apply periodic boundary conditions in the b direction, to reduce finite-size effects. Then, from Fig. 1, we can use a chain description in which the classical energy per spin is

$$\mathcal{E}(\{\phi_l\}) = \frac{1}{L}\sum_{l=1}^{L}[4J_1S^2\cos(\phi_l - \phi_{l+1})$$
$$+ 2J_1'S^2\cos(\phi_l - \phi_{l+2}) - g\mu_B HS\cos\phi_l]; \quad (4)$$

the chain-site index l runs in the b direction, ϕ_l is the angle between $\mathbf{S}_l$ and the field, and the chain length L is a multiple of 3. Equation (4) is just the classical energy per spin for the

axial next-nearest-neighbor Heisenberg chain, except for the restriction on L. The optimal solutions are never TAFM states, but they have related features, and so we use also the representation $\phi_{i,l'} \equiv \phi_{3l'+i}$ where $i = 1, 2$, and 3 is the sublattice index.

The Euler-Lagrange equations are obtained from $\partial\mathcal{E}/\partial\phi_l = 0$:

$$4J_1S^2[\sin(\phi_l - \phi_{l+1}) - \sin(\phi_{l-1} - \phi_l)]$$
$$+ 2J_1'S^2[\sin(\phi_l - \phi_{l+2}) - \sin(\phi_{l-2} - \phi_l)]$$
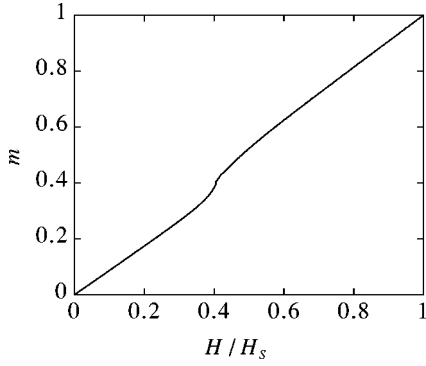$$= g\mu_B HS\sin\phi_l. \quad (5)$$

These are L coupled, nonlinear difference equations with boundary conditions $\phi_{l+L} = \phi_l(\mathrm{mod}\,2\pi)$. It is not in general legitimate to approximate them by differential equations; doing so would miss the sequences of C states that we find at both low and high fields.

Equation (5) has several analytical solutions, namely, the zero-field helical state $\phi_l = ql$, the aligned state $\phi_l \equiv 0$, and the TAFM states described by Eq. (3) with J_1 replaced by $\bar{J} \equiv (2J_1 + J_1')/3$. Analytical progress is possible for small fields and for H just below H_S.[13] In general Eq. (5) must be solved numerically; this led us to previously unknown solutions. The equations have in fact a multitude of solutions. This multiplicity results in part from a degeneracy not present in systems (such as $CsCuCl_3$) where the IC phase is driven by a Dzyalshinskii-Moriya interaction. In $RbCuCl_3$, both right- and left-handed helices are degenerate in energy, at nonzero field as well as at $H = 0$ (where the relation $\cos q_0 = -J_1/2J_1'$ determines only the magnitude of q_0). The multiplicity results also from the many possible periods for fixed winding number N (defined below).

We solved the equations by Newton's method, starting from approximations obtained by various means (for example, solutions at a nearby field), using periods L up to $\approx 3 \times 10^4$ for several dozen values of N up to 2103; we linearized the equations about the starting values and solved the linear equations to obtain the corrections, repeating the procedure until the root-mean-square residual was less than 10^{-11} or so. The field range from 0 to H_S was covered in increments of $\Delta H \approx 2 \times 10^{-4} H_S$. Properties of the IC states (such as the optimal chain length, the energy, and the magnetization) are easily obtained by interpolation; for this purpose it is useful to work with lengths corresponding to many periods. Periodic boundary conditions necessarily give structures with rational periods, but inspection usually suffices to distinguish commensurate from incommensurate structures.

III. MAGNETIC STRUCTURES

The effect of a transverse magnetic field on helical spin structures arising from competing exchange interactions, such as described by the classical Hamiltonian in Eq. (4), was studied analytically in detail by Nagamiya et al.[13] They found a distorted helical phase at low fields and an IC-fan phase at high fields. In the latter, the spins oscillate about the field direction; the oscillations decrease with increasing field, vanishing continuously at H_S. If the transition from the low-

FIG. 2. The field dependence of the reduced magnetization m.

FIG. 3. The order parameter [the angles $\phi_{i,l'}$ in the three-sublattice representation, as defined below Eq. (4)] in the helical phase at $H=0.33H_S$.

field helical phase occurs directly to the high-field fan phase, then it is first order. Reference 13 gives the variational estimate $H_c/H_S=\sqrt{(1+\beta)(2+\beta)}-(1+\beta)$, with $\beta=(1-J_1/J_1')^2$, for the transition field H_c; for RbCuCl$_3$, one finds $H_c=0.423H_S$ on using the parameters given below Eq. (1). Reference 13 found also that other structures can be optimal at intermediate fields, depending on the ratio J_1/J_1'; in particular, for $J_1/J_1'\lesssim1$ as in RbCuCl$_3$, and for fields near $\frac{1}{2}H_S$, the energy of a TAFM state lies below the analytical estimates for both of these IC phases.

Our numerical solution of the Euler-Lagrange Eq. (5) gives the helical IC and fan IC phases at small and large fields, respectively, as in Ref. 13. Our results differ qualitatively however at intermediate fields, from $H=0.29H_S$ to $0.64H_S$. For $0.29<H/H_S<0.41$, we find many helical commensurate (C) phases not previously known in this context. These are not TAFM states (with period 3 in the chain description) but rather lock-in phases with larger periods; they alternate with the helical IC phase, and within our field resolution ($\Delta H\approx2\times10^{-4}H_S$) eventually supplant it completely. The behavior is similar in some respects to that found in the axial, next-nearest-neighbor Ising model.[16] At $H=0.41H_S$, a first-order transition occurs to a previously unknown, second IC phase (we call it the IC2 phase); this appears to be the transition observed in Ref. 8. Two weaker first-order transitions follow swiftly, to a third IC phase (the IC3 phase, also previously unknown) and then to fan phases; the latter are predominantly IC, but we find also a sequence of lock-in phases each optimal over a small field interval. Finally, there is a second-order transition to the aligned phase; we derive an analytical expression for the saturation field, in terms of the parameters in the Hamiltonian.

Figure 2, our main result, shows the field dependence of the reduced magnetization

$$m=\frac{1}{L}\sum_{l=1}^{L}\cos,\phi_l. \qquad (6)$$

A discontinuity ($\Delta m\approx9\times10^{-3}$) occurs at $H=0.405H_S$; this field is however somewhat larger than the $H=0.32H_S$ where a magnetization jump is found experimentally,[8] and
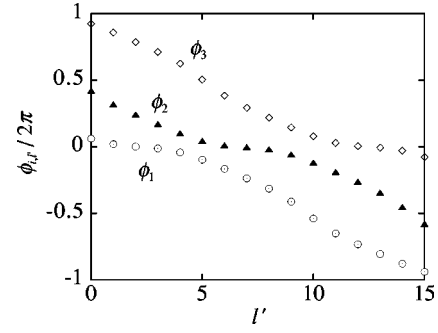
there is a lot of fine structure not reported in Ref. 8. We now describe the phases in more detail.

A. Low-field region: $0<H<0.405H_S$

The structures are helical, with three equivalent sublattices; each sublattice phase winds through 2π a total of $N/3$ times, where the total winding number N is a multiple of 3, like the chain length L. The helical phase can be treated analytically at small H, as in Ref. 13. The magnetic field distorts the zero-field spin structure $\phi_l=q_0l$, modulating the phases. In weak fields,

$$\phi_l\approx ql+a\sin ql, \qquad (7)$$

where the optimal amplitude a and wave number q are field dependent; they are determined so as to minimize the energy $\mathcal{E}$. As the magnetic field is increased, the spin structure distorts further as higher harmonics are generated. Figure 3 shows the order parameters (the angles $\phi_{i,l'}$ in the three-sublattice representation) found from numerical solution of Eq. (5) at $H=0.33H_S$.

The wave number q of the helical phase is

$$q=\frac{2\pi}{3}\left(1-\frac{N}{L}\right), \qquad (8)$$

in terms of the total winding number N and the chain length L; one must distinguish between q and the wave number $2\pi N/L$ of the chain. From Fig. 4, at low fields q increases
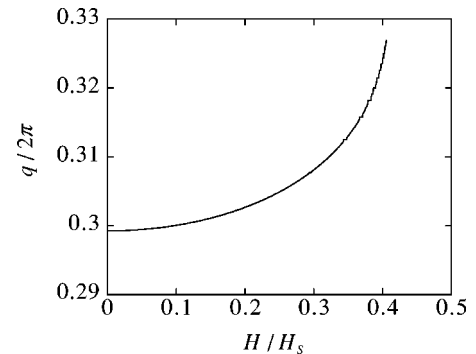
FIG. 4. The field dependence of the wave number q in the low-field region $0<H<0.405H_S$.
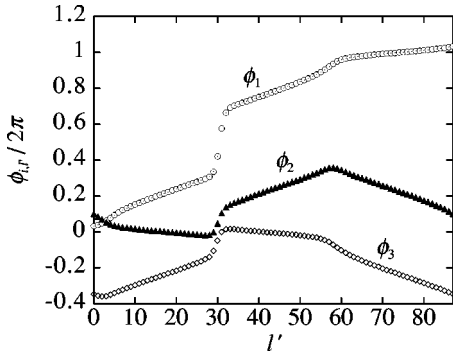
FIG. 5. The angles $\phi_{i,l'}$ in the IC2 phase at $H=0.41H_S$.

FIG. 6. The angles $\phi_{i,l'}$ in the IC3 phase at $H=0.424H_S$.

with the field, initially quadratically, as the higher harmonics grow. At $H=0.293H_S$, however, a lock-in transition takes place to a helical C phase with $L/N=13$; this phase extends to $H=0.296H_S$ where the helical IC phase becomes optimal again. Other lock-ins occupying comparable field intervals occur at $L/N=16$, 19, etc. in steps of 3, up to $L/N=52$ at the transition to the IC2 phase. Minor lock-ins (occupying much smaller field ranges) occur at $L/N=29/2$, 35/2, 18, 20, 41/2, 21, 85/4, 91/4, 23, 47/2, 24, 53/2, 59/2, and 65/2; others likely exist but require a finer field step to be detected. Windows of the helical IC phase exist at higher fields, but they eventually become too narrow to detect (at our field step) and we see a staircase of C states which terminates at $H=0.405H_S$ in a first-order transition ($\Delta m\approx9\times10^{-3}$) to the IC2 phase.[17]

B. IC2 phase

This phase is optimal in the very narrow range $0.405<H/H_S<0.419$. Figure 5 shows the order parameters at $H=0.410H_S$. The structure resembles that of the helical phase (as shown in Fig. 3); the three sublattices are however no longer equivalent, for the spins on only one of them wind through 2π (rather than all three as in the helical phase). The optimal chain period increases monotonically with the field, from ≈180 to ≈1800 at the transition to the IC3 phase; the latter transition is weakly first order, with $\Delta m\approx8\times10^{-4}$.

C. IC3 phase

This phase is also optimal over only a very small field range, $0.419<H/H_S<0.428$. The three sublattices are inequivalent, as in the IC2 phase, but here none of the three winds through 2π. Figure 6 plots the order parameters at $H=0.424H_S$; one sees that the IC3 phase is a rippled commensurate phase, in which the order parameter oscillates about a particular TAFM state. The IC3 state can be expressed in terms of the amplitude a_i and the phase δ_i of the oscillation on the ith sublattice as

$$\phi_{i,l'}\approx\phi_i+a_i\sin\left[\frac{2\pi l'}{(L/3)}+\delta_i\right],\qquad(9)$$

where $\phi_1=\phi_3$; the amplitudes are zero for the TAFM state in question. As the field increases, the oscillations become smaller and the period L increases (from ≈80 to ≈260);
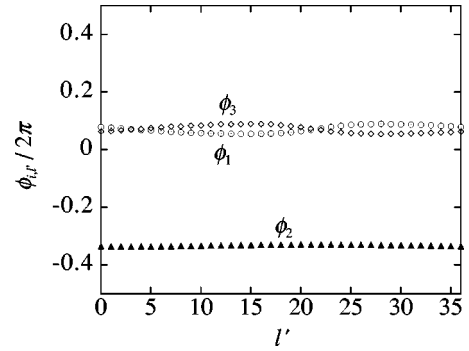
correspondingly, the TAFM state becomes more favorable, but before it becomes optimal there occurs a very weak first-order transition ($\Delta m\approx2\times10^{-5}$) to the fan phase. The IC3 phase (like the IC2 phase) requires a full numerical solution of Eq. (5); it should be possible however to demonstrate analytically that the TAFM state becomes unstable to these perturbations at some field greater than $0.428H_S$ (the upper limit of the IC3 phase).

We point out a remarkable connection with the theory of fluctuations in the TAFM.[14,15] Both thermal and quantum fluctuations break the classical degeneracy in the same way; for $H>\frac{1}{3}H_S$, two angles are identical in the optimal state, say, $\phi_1=\phi_3$.[14,15] Our point is that this same state serves as the basis for the IC3 state in RbCuCl$_3$; the lattice distortion induces the spins to fluctuate spatially, and the energy is minimized when the fluctuations occur about the state with two angles identical, just as for thermal and quantum fluctuations.

D. High-field region: $0.428H_S<H<H_S$

As shown in Fig. 7, the spins oscillate about the field direction, without winding through 2π; the three sublattices are again equivalent. The amplitude of the oscillation decreases as H increases, going to zero at the transition, at H_S, to the aligned phase.

The wave number q in this region is obtained from the chain period L as

$$q=(2\pi/3)(1-3/L).\qquad(10)$$
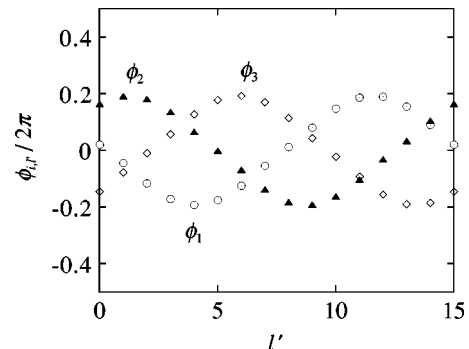
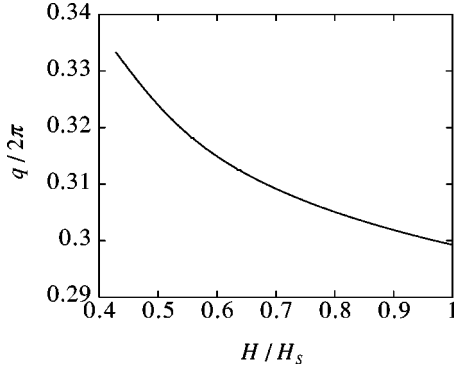FIG. 7. The angles $\phi_{i,l'}$ in the fan phase at $H=0.5H_S$.

FIG. 8. The field dependence of the wave number q in the high-field region $0.428H_S < H < H_S$.

As the field increases, the optimal chain length decreases from an estimated value greater than 10^5 at the IC3-fan transition, to the interpolated value ≈ 29.4 at H_S. Correspondingly q decreases monotonically from $\approx 2\pi/3$ to ≈ 1.88 ($\approx 2\pi \times 0.299$); Fig. 8 gives numerical values. The structure is incommensurate in most of the fan region, but we find also narrow lock-in phases; these are less prominent than in the helical region at low fields. The widest C phase, with $L/3 = 16$ and width $0.006H_S$, occurs near $0.64H_S$. Seven others occur at smaller H, at $L/3 = 22$, 28 etc.; smaller field steps would likely find many more.

The transition at H_S is second order and so the fan phase can be treated analytically in this region, as in Ref. 13. Expanding the energy function $\mathcal{E}$ in ϕ_l, one finds

$$\mathcal{E} = S^2(4J_1 + 2J_1' - g\mu_B H/S)$$
$$+ \frac{S^2}{2L}\sum_l \{[g\mu_B H/S - (8J_1 + 4J_1')]\phi_l^2$$
$$+ 8J_1\phi_l\phi_{l+1} + 4J_1'\phi_l\phi_{l+2}\} + O(\phi^4). \quad (11)$$

Introducing the Fourier transform $\phi_l = 1/\sqrt{L}\sum_q \phi_q e^{iql}$, one can write Eq. (11) as

$$\mathcal{E} = S^2(4J_1 + 2J_1' - g\mu_B H/S)$$
$$+ \frac{S^2}{2L}\sum_q \{g\mu_B H/S - 2[J(0) - J(q)]\}|\phi_q|^2 + O(\phi^4),$$
$$\quad (12)$$

where $J(q) \equiv 4J_1\cos q + 2J_1'\cos 2q$. Obviously the optimal state of Eq. (12) is given by $\phi_q = 0$ for all q if $H > H_S = 2[J(0) - J(q_0)]S/g\mu_B$, where q_0 gives the minimum value of $J(q)$, i.e., $\cos q_0 = -J_1/2J_1'$. Surprisingly, the optimal IC wave number in the limit $H \to H_S$ is identical to the value at $H = 0$, even though the structures are quite different. Our analytical result

$$H_S = (8J_1 + 2J_1^2/J_1' + 8J_1')S/g\mu_B \quad (13)$$

evaluates to $H_S = 66$ T on using the parameter values given below Eq. (1). For $H \lesssim H_S$, the optimal solution is given by

$$\phi_l \approx a\cos(q_0 l + \delta), \quad (14)$$

where δ is an arbitrary phase; the optimal amplitude a is determined by taking into account the fourth-order terms in the energy function $\mathcal{E}$.

The difference between our result (13) and the field $(12J_1 + 6J_1')S/g\mu_B$ (below which the aligned state is unstable with respect to TAFM states) is $2(J_1 - J_1')^2 S/g\mu_B J_1'$. It is then obvious that the transition at H_S with decreasing field is to a modulated state, except in the spatially isotropic case $J_1' = J_1$. The TAFM states are then rather fragile. They are unstable also at $H = 0$ when $J_1' \neq J_1$, and we show above that they are never optimal for the anisotropy appropriate to RbCuCl₃; it remains to be determined whether they survive at intermediate fields for general anisotropy.

By using the classical approximation, we have omitted the effects of quantum fluctuations. One can argue that quantum fluctuations are not important for RbCuCl₃, for their effect in CsCuCl₃ in transverse field is to give rise to a plateau in the IC wave number,[20] rather than a new phase. On the other hand, quantum and thermal fluctuations in CsCuCl₃ stabilize states that are otherwise not optimal, in longitudinal[2] and transverse[6] fields, respectively. We made a preliminary effort to understand the effects of quantum fluctuations, using a biquadratic term in the energy.[20] Not unexpectedly, we find that the magnetization develops plateaus, in conflict with experiment on RbCuCl₃, but we did not search extensively for other states. We note however that such a plateau has recently been reported[21] in the distorted triangular antiferromagnet Cs₂CuBr₄; it appears that fluctuations are more important here than in RbCuCl₃.

IV. SUMMARY

The classical theory of spin structures of RbCuCl₃ in a transverse magnetic field is surprisingly rich. We found four IC phases and as well two series of C phases. We showed that the wave number of the helical IC phase at $H = 0$ is identical to that of the fan IC phase as $H \to H_S$, and we pointed out a remarkable connection between one of the IC phases and the effects of thermal and quantum fluctuations in the TAFM. We showed that the TAFM states of the isotropic case are fragile; infinitesimal anisotropy makes them nonoptimal at both small and large fields, and they are nonoptimal at all fields for RbCuCl₃. We found that the magnetization is discontinuous at $H \approx 0.41H_S$, in qualitative agreement with experiment. Direct observation of the two intermediate IC phases and the C phases will be difficult; they occupy only small field intervals, and the large value of H_S requires demanding pulsed experiments. Our predictions for the structure of the high-field fan phase are likely more easily tested.

[1] A review is given by M. F. Collins and O. A. Petrenko, Can. J. Phys. **75**, 605 (1997).

[2] H. Shiba and T. Nikuni, *Recent Advances in Magnetism of Transition Metal Compounds*, edited by A. Kotani and N. Suzuki (World Scientific, Singapore, 1993), p. 372; T. Nikuni and H. Shiba, J. Phys. Soc. Jpn. **62**, 3268 (1993).

[3] M. Motokawa, M. Arai, H. Ohta, M. Mino, H. Tanaka, and K. Ubukata, Physica B **211**, 199 (1995).

[4] T. Werner, H. B. Weber, J. Wosnitza, A. Kelnberger, M. Meschke, U. Schotte, N. Stüßer, Y. Ding, and M. Winkelmann, Solid State Commun. **109**, 609 (1997).

[5] U. Schotte, A. Kelnberger, and N. Stüßer, J. Phys.: Condens. Matter **10**, 6391 (1998).

[6] A. E. Jacobs and T. Nikuni, J. Phys.: Condens. Matter **10**, 6405 (1998).

[7] Y. Tazuke, S. Kinouchi, H. Tanaka, K. Iio, and K. Nagata, J. Phys. Soc. Jpn. **55**, 4020 (1986).

[8] S. Maruyama, H. Tanaka, Y. Narumi, K. Kindo, H. Nojiri, M. Motokawa, and K. Nagata, J. Phys. Soc. Jpn. **70**, 859 (2001).

[9] M. Reehuis, R. Feyerherm, U. Schotte, M. Meschke, and H. Tanaka, J. Phys. Chem. Solids **62**, 1139 (2001).

[10] W. J. Crama, J. Solid State Chem. **39**, 168 (1981).

[11] M. Harada, J. Phys. Soc. Jpn. **52**, 1646 (1983).

[12] T. Kato, K. Iio, T. Hoshino, T. Mitsui, and H. Tanaka, J. Phys. Soc. Jpn. **61**, 275 (1992), observed a similar IC structure in $RbMnBr_3$, but here the intrachain exchange interaction appears to be antiferromagnetic.

[13] T. Nagamiya, K. Nagata, and Y. Kitano, Prog. Theor. Phys. **27**, 1253 (1962).

[14] H. Kawamura, J. Phys. Soc. Jpn. **53**, 2452 (1984).

[15] A. V. Chubukov and D. I. Golosov, J. Phys. Condens. Matter **3**, 69 (1991).

[16] P. Bak, Rep. Prog. Phys. **45**, 587 (1982).

[17] The susceptibility grows rapidly at fields just below the discontinuous transition to the IC2 phase, suggesting an interrupted second-order transition. Inspection of the numerical solutions in this field region shows that the order parameter lacks the characteristics of transitions of instability type (and so we doubt that a bicritical point lies nearby in parameter space), nucleation type, or intermediate type, as discussed, for example, in Ref. 18. Between passages through $\phi = \pi$, the order parameter is the spatially varying commensurate state (Ref. 19) first described for the classical IC phase of $CsCuCl_3$. This state occurs in both $RbCuCl_3$ and $CsCuCl_3$, and also in another model (Ref. 18), because the commensurate state is continuously degenerate. Quantum and thermal fluctuations break the TAFM degeneracy and so may become important (Refs. 20 and 6) in this field region.

[18] T. Ohyama, A. E. Jacobs, and D. Mukamel, Phys. Rev. E **53**, 2595 (1996).

[19] A. E. Jacobs, T. Nikuni and H. Shiba, J. Phys. Soc. Jpn. **62**, 4066 (1993).

[20] T. Nikuni and A. E. Jacobs, Phys. Rev. B **57**, 5205 (1998).

[21] H. Tanaka, T. Ono, H. Aruga Katori, H. Mitamura, F. Ishikawa, and T. Goto, Prog. Theor. Phys. Suppl. (to be published).